Macromolecules

Article

pubs.acs.org/Macromolecules

Lateral Structure Formation in Polyelectrolyte Brushes Induced by Multivalent Ions

Blair Brettmann,[†] Philip Pincus,[‡] and Matthew Tirrell*[,†,§]

[†]The Institute for Molecular Engineering, The University of Chicago, 5640 S. Ellis Ave., Chicago, Illinois 60637, United States

[‡]Materials Department, Room 3004 Materials Research Laboratory, University of California, Santa Barbara, Santa Barbara, California 93106, United States

[§]The Institute for Molecular Engineering, Argonne National Laboratory, 9700 Cass Avenue, Lemont, Illinois 60439, United States

ABSTRACT: We provide a theoretical model for the collapse of polyelectrolyte brushes in the presence of multivalent ions, focusing on the formation of lateral inhomogeneties in the collapsed state. Polyelectrolyte brushes are important in a variety of applications, including stabilizing colloidal particles and lubricating surfaces. Many uses rely on the extension of the densely grafted polymer chains from the surface in the extended brush morphology. In the presence of multivalent ions, brushes are significantly shorter than in monovalent ionic solutions, which greatly affects their properties. We base our theoretical analysis on an analogous collapse of polyelectrolyte brushes in a poor solvent, providing an energy balance representation for pinned micelles and cylindrical bundles. The equilibrium brush heights predicted for these structures are of a similar magnitude to those measured experimentally. The formation of lateral structures can open new avenues for stimuli-responsive applications that rely on nanoscale pattern formation on surfaces.

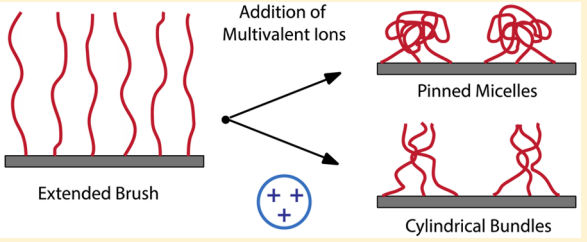

INTRODUCTION

Interfacial layers of polymers formed via end tethering of chains to a surface have found significant utility in a variety of technological applications and have been a valuable system for fundamental scientific studies. At high tethering densities, the chains crowd one another, resulting in strong deformations that lead to stretching away from the surface. This strongly stretched brush morphology is key to the unique properties of polymer brushes, such as their ability to stabilize colloidal dispersions[1] and their superior lubrication properties.[2] However, the brush morphology is sensitive not only to grafting density but also to the local environmental conditions, and morphologies other than the extended brush are expected to form as the environment is changed, for example, in poor solvents, at low temperatures, and in the presence of multivalent salts.[3] The formation of the new morphologies can affect the behavior of the brush in technological applications,[4] lead to exciting new functional materials,[5] and serve as a model for developing a deeper understanding of polymer physics in these environments.

A class of polymer brushes, polyelectrolyte brushes, consists of charged polymers end tethered to surfaces. These materials add a new mechanism for environmental response and a new layer of complexity due to long-ranged electrostatic interactions. They are an important class of materials, both from a technological standpoint, as they are used frequently in colloidal stabilization, lubrication, drug delivery, coatings, and adhesives, and from a biological perspective, as they appear naturally in many living organisms.[6,7]

Pincus[1] and Borisov et al.[8] provided initial theoretical studies of a planar, strong polyelectrolyte brush in the absence of added salt, demonstrating that counterions are confined within the brush layer to maintain electroneutrality. In addition to steric effects from the dense packing, the extension of the polyelectrolyte brush is affected by the polymer charges and the counterions, with the entropy of the confined counterions providing a dominating force leading to strong stretching. Since those seminal works, significant efforts have expanded the understanding of polyelectrolyte brushes to include monovalent ion salt solutions, poor solvents, weak polyelectrolytes, and curved surface geometries, and a variety of experimental, simulation, and theoretical techniques have been employed to study these systems.[9]

We are interested in a less well-studied environment for the polyelectrolyte brush, multivalent salt solutions. Multivalent ions are prevalent in industrial formulations and biological fluids, and a fundamental understanding of the interaction of a polyelectrolyte brush with simple multivalent ions can pave the way for understanding of more complex multivalent species, such as proteins, other polyelectrolytes, and surfactants. Experimental studies have shown that polyelectrolyte brushes undergo a sharp collapse in the brush height as the concentration of multivalent ions is increased.[10−14] This is similar to the observed phenomenon of polyelectrolyte precipitation in multivalent ion solutions[15−17] and structure

Received: November 27, 2016
Revised: December 31, 2016

DOI: 10.1021/acs.macromol.6b02563
Macromolecules XXXX, XXX, XXX−XXX

formation in star polyelectrolytes induced by multivalent ions,[18,19] but with additional constraints due to the end-tethering. Early theoretical treatments proposed that the collapse is driven by the decrease in the osmotic pressure on replacing multiple monovalent counterions by a single multivalent ion,[14] but while it is an important contribution to lower brush heights, it is insufficient to fully explain brush behavior in multivalent ion solutions.

In our previous study, we added a consideration for counterion condensation and ionic bridging to a simple energy balance for the polyelectrolyte brush in the presence of multivalent ions.[20] The ability of a single multivalent ion to condense onto two separate polyelectrolyte chains and form an ionic cross-link is expected to contribute to the sharp collapse of the brush height when sufficient bridges have been formed. This is supported in part by the observation of an attractive force between opposing brushes when they are pulled apart in the presence of multivalent ions, as measured using the surface force apparatus.[10] To further investigate the collapse of the polyelectrolyte brush in the presence of multivalent ions, we aim to improve on our previous model and capture the morphology of the collapsed brush state.

Our previous model assumed a step function concentration profile and a brushlike morphology in the collapsed as well as extended brush state. The model was based on an energy balance containing the virial terms, the polymer chain elasticity, the entropy of the free counterions, and the entropy of the condensed counterions, with additional parametrized phenomenological terms for the counterion condensation and bridging.[20] While this representation of the system approximated the phenomenon of the extended brush height and sharp collapse well, it greatly underestimated the collapsed state brush height. For parameters similar to the experimental systems, the collapsed state brush height was approximately 0.07 nm, while the experimental result was approximately 30 nm. This led to the conclusion that a model that allows for lateral inhomogeneities in polymer density may be more appropriate to describe the collapse.

In developing a new model for the collapsed state of the polyelectrolyte brush, the electrostatic attractions from bridging can be considered as analogous to short-range attractions between monomers for a polymer in a poor solvent. This same type of analogy has been used to describe collapse of polyelectrolytes at low temperatures due to dipole−dipole interactions.[21] Prior studies of brush collapse in the presence of a poor solvent have shown structures other than a homogeneous collapsed brush.[22−26] A few of the structures and the terminology used to describe them are illustrated in Figure 1.

The "dimple" structure is difficult to approximate with a simple model due to strong heterogeneities in both the vertical and lateral direction, so this work focuses on the pinned micelle and bundle structures. The pinned micelles were originally described for neutral polymer brushes in a poor solvent by Williams (called octopus micelles in that work)[22] and extended to polyelectrolyte brushes in a poor solvent by Zhulina.[23] Bundle formation for a neutral polymer brush in a poor solvent was examined by Ross and Pincus but found to be unfavorable in the single brush case.[26] It was found, however, that bundle formation may occur in a brush that is tethered at both ends. For a polyelectrolyte brush, Carrillo and Dobrynin[27] and He et al.[28] showed through simulations and scaling theory that bundle

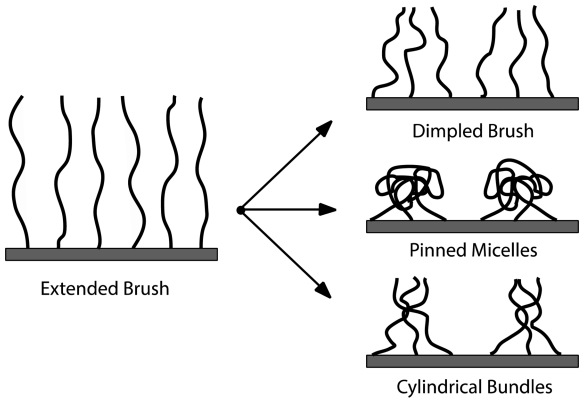

Figure 1. Illustration of extended brush and three types of laterally inhomogeneous structures, dimples, pinned micelles, and bundles.

formation may occur for polyelectrolyte brushes in a poor solvent.

In addition to noting that the short-range attractions in these poor solvent models are similar to the bridging interactions in polyelectrolyte brushes in multivalent ionic solutions, we can also compare polymer density profiles from experiments on collapsed polyelectrolyte brushes in multivalent salt solutions to calculated density profiles from poor solvent models. The experimental scattering length density profile measured via neutron reflectivity for polystyrenesulfonate brushes with trivalent counterions presents a shape close to a Gaussian function, rather than the parabolic form typically found for polyelectrolyte brushes.[12] This density profile is very similar to that predicted by Zhulina et al. for polyelectrolyte brushes in poor solvents.[23]

Though our previous model captures the phenomenological collapse of the brush, it predicts a collapsed state brush height that is much lower than found experimentally (0.07 nm vs 30 nm). In this work, we aim to develop a more accurate simple representation for the collapsed brush state, basing our theory on studies of polymer and polyelectrolyte brushes in poor solvents.[22,23,27] We examine both a pinned micelle structure (Figure 2A) and a cylindrical bundle structure (Figure 2B).

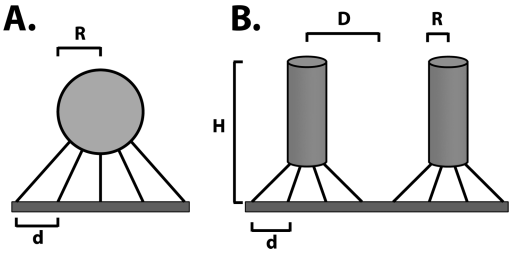

Figure 2. Illustration of the geometry of the pinned micelle (A) and cylindrical bundle (B) structures with key size parameters of *d*, the grafting spacing, *R*, the structure radius, *D*, the distance between structures and *H* the height of the cylindrical bundles.

THEORETICAL APPROACH

Pinned Micelle Structure. When a polymer chain in solution collapses in a poor solvent, it will form a dense spherical structure, and in a nondilute polymer solution these spheres can contain contributions from multiple polymer chains. This same concept can be applied to polymer brushes, but the end-tethering of the chains limits the structure that can

DOI: 10.1021/acs.macromol.6b02563
Macromolecules XXXX, XXX, XXX−XXX

form. At low grafting densities, the polymers contract into a single globule per polymer chain, while at very high densities, the chains are so close-packed that a uniform layer will form. At intermediate grafting densities, however, pinned micelles will form. The pinned micelle structure consists of a number of chains, n, bundled together to form a spherical structure on the grafting surface, where the chains are still pinned at one end (termed "legs").[22]

We consider a brush made of long, flexible chains tethered to a planar solid surface with a grafting spacing d. The polymer contains N monomers per chain, and the monomers and ions, as well as the distance between neighboring monomers, are of size a, whose value is set to 0.25 nm. All lengths in the model are normalized by this monomer size a and thus are dimensionless. Unlike the homogeneous brush model, we do not consider the brush in the extended state, and there is no explicit multivalent ion concentration dependence of the model. Instead, we assume the brush is in an environment containing only the multivalent counterions and no added salt, providing sufficient multivalent ions to lead to collapse, but not such a high concentration as to lead to re-entrant behavior.

To develop a model for multivalent ion-driven polyelectrolyte brush collapse that is analogous to a collapsed brush in a poor solvent, we start with the pinned micelle model proposed by Williams for a neutral polymer brush in a poor solvent.[22] The free energy of the pinned micelle can be approximated by a balance of the surface tension and the leg stretching (from the legs stretching to the micelle) on a per chain basis (all free energy expressions are on a per chain basis unless otherwise specified).

$$\frac{F}{kT} \approx \frac{F_{surf}}{kT} + \frac{F_{leg}}{kT} \tag{1}$$

The formation of pinned micelles is governed by the gain in the surface free energy per chain in a micelle composed of multiple chains rather than individual globules on the surface. This is countered by the penalty for the chains to stretch due to the constraint that they are irreversibly pinned to the grafting surface.

The radius of the pinned micelle can be approximated by the radius of the "polymer chain" (the total number of monomers that make up the micelle or approximately nN) in a poor solvent:

$$R = (nN/\tau)^{1/3} \tag{2}$$

where τ is a parameter for the solvent quality and is related to the second virial coefficient, ν, by $\nu = -\tau$ and $\tau = (\theta - T)/\theta$.[23]

The surface tension term is based on the surface tension per chain at the boundary between the pinned micelle sphere and solvent. The pinned micelle sphere can be represented as a sphere of N_b densely packed thermal blobs of size $\xi \approx 1/\tau$. The surface free energy can be estimated as kT per each surface blob. The number of these surface blobs is approximately $(2R)^2/\xi^2$. Neglecting numerical prefactors, this makes the surface tension contribution per chain, when normalized by kT:[23]

$$\frac{F_{surf}}{kT} \approx \frac{R^2}{\xi^2 n} = \frac{\tau^2 R^2}{n} = \frac{N^{2/3}\tau^{4/3}}{n^{1/3}} \tag{3}$$

To characterize the leg stretching penalty, the pinned micelle is approximated as a stretched globule due to the propensity of the polymer to collapse into a globule combined with the stretching from the constrained chain ends. Halperin and Zhulina previously showed that a deformed globule can exist as a weakly deformed globule and a stretched string of blobs (as opposed to a strongly stretched ellipsoidal globule),[29] which is how we represent the pinned micelle.

For the stretched globule with an end-to-end distance $D \gg R$, the globule consists of a chain of n_L thermal blobs of length $L_{chain} = n_L\xi$ and a spherical core $R \approx ((N - n_L\xi^2)/\tau)^{1/3}$. This is illustrated in Figure 3.

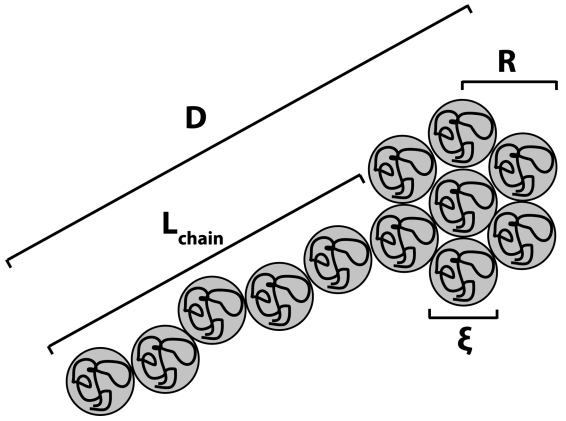

Figure 3. Illustration of a stretched globule composed of thermal blobs.

For the level of stretching that occurs for pinned micelles, the size of the core is much less than the length of the chain of thermal blobs, $R \ll L_{chain}$, so the end-to-end distance of the globule is approximately equal to the length of the chain of thermal blobs, $D \approx L_{chain}$.[30] We are therefore developing an equation for the free energy of a stretched chain of some number of blobs that make up all the legs in the micelle. For a pinned micelle of n chains, we calculate the average length of a leg based on the assumption that $D \approx L_{chain}$.

The total length of all chains in the pinned micelle can be estimated as the volume of the zone the chains are stretching over divided by the area between chains (i.e., d^2):

$$nL_{chain,sum} \approx \frac{1}{d^2}\frac{1}{2}\int_0^{R_c} dr\, r^2 \approx \frac{1}{2}\frac{1}{d^2}D^3 \tag{4}$$

The radius of the zone covered by the pinned micelle, $D \approx (nd^2)^{1/2}$ (from $n \approx$ area of stretching zone/area between chains, $n \approx D^2/d^2$). Thus, the total length of all chains in the pinned micelle is

$$nL_{chain,sum} \approx \frac{1}{2}\frac{1}{d^2}(nd^2)^{3/2} \tag{5}$$

or the average length of the leg can be estimated as

$$L_{chain} \approx D \approx (nd^2)^{1/2} \tag{6}$$

Estimating the free energy of the stretched globule, and hence the stretching of the leg, to be on the order of kT per blob, the elastic stretching penalty can then be approximated as

$$\frac{F_{leg}}{kT} \approx n_L \approx \frac{D}{\xi} \approx \tau D = \tau(nd^2)^{1/2} \tag{7}$$

This is already on a per chain basis because D is the average length of a leg not a sum of all lengths. For neutral polymers, F_{surf} and F_{leg} balance one another to achieve an equilibrium

DOI: 10.1021/acs.macromol.6b02563
Macromolecules XXXX, XXX, XXX−XXX

number of chains in the pinned micelle and hence the pinned micelle size.

For charged polymers, the electrostatics must also be taken into account, leading to

$$\frac{F}{kT} \approx \frac{F_{surf}}{kT} + \frac{F_{leg}}{kT} + \frac{F_{elec}}{kT} \tag{8}$$

The expressions for F_{surf} and F_{leg} are the same as for the neutral brush. The appropriate expression for F_{elec} is less clear. In general, electrostatic interactions between chains will lead to repulsion between chains that disrupts the micelles and favors an extended brush. In addition, any counterions that are trapped within the brush but not condensed would give rise to an osmotic pressure that further drives the formation of an extended brush, though at this stage we are assuming no osmotically active counterions in the collapsed state. At this point, we are also not considering multivalent ion effects (i.e., bridging) as part of the F_{elec} term. Despite the anticipated effects of charged monomers on the state of the brush, it has been shown that in the collapsed state, few monomers remain charged and the dense collapsed brush may behave as an amorphous ionic solid.[17] In this work, we examine two different models for the electrostatics of the collapsed state.

The first representation was proposed by Zhulina et al. for polyelectrolyte brushes in poor solvents.[23] They assumed a core composed of charged polymer chains with $q = fN$ immobilized charges and q mobile counterions in the solution, similar to a charged liquid droplet. The charge fraction, f, is the fraction of polymer charges not containing condensed counterions, or the exposed charged monomers. This is illustrated in Figure 4A.

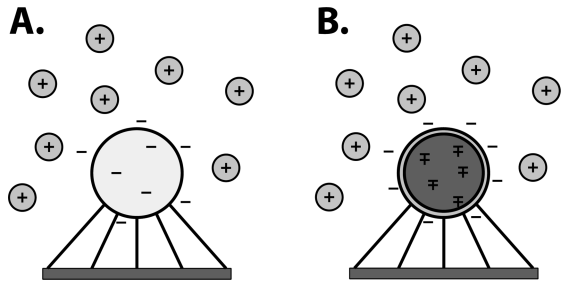

Figure 4. (A) Illustration of the charged liquid droplet representation for the electrostatics with consideration only for the remaining polymer charges in the energetics. (B) Illustration of the ionic solid representation for the electrostatics with consideration for the remaining polymer charges and the formation of a charge-compensating dense solid in the energetics.

The free energy in this model is dominated by the increase in unscreened Coulomb repulsion between the charges on the polymer chains inside the micelle core. The cluster energy on a per chain basis is described by the Coulomb repulsion of the charges in the cluster:

$$\frac{F_{elec}}{kT} \approx l_B(fN)^2 n/R \tag{9}$$

where R is the radius of the spherical cluster and $l_B = e^2/(4\pi\varepsilon_0\varepsilon_r kT)$.

The effect of the electrostatic interactions falls into two regimes: when $F_{leg}/F_{elec} \gg 1$, the micelles are essentially neutral and the free energy can be approximated by the balance of F_{leg} to F_{surf}, and when $F_{leg}/F_{elec} \ll 1$, the electrostatics play a large role and the free energy can be approximated as a balance between F_{surf} and F_{elec}.[23]

On the basis of this representation for F_{elec}, Zhulina et al. demonstrated that the pinned micelles are favored at low charge fractions, but the extended brush is favored at higher charge fractions. This crossover point occurs at

$$f^* \approx (\tau d^2)^{1/2}/N \tag{10}$$

For similar parameters to our system ($d = 40$, $N = 1000$, $\tau = 0.9$), the polymer charge fraction above which the brush transitions from pinned micelles to homogeneous extended brush is $f^* \approx 0.02$. Clearly this is a low charge fraction and would lead to a favorable collapsed state only at a high degree of counterion condensation. One reason for this conclusion is that there is no electrostatics term that leads to a favorable collapsed state; we only include the repulsion of the remaining charges. An alternate electrostatics model for this system adds an additional term for the favorability of forming an amorphous ionic solid with the negative polymer charges and positive ion charges arranged in a tight, charge compensating solid, as illustrated in Figure 4B.

Solis et al. approached the problem of polyelectrolyte collapse in solutions of multivalent ions, providing an estimate for the free energy of the collapsed state as well as the extended polymer state.[17] This differs somewhat from our situation in that we have additional restrictions and energy contributions due to the tethering but may be expected to display similar electrostatics. The model provides separate energy functions for the collapsed and extended state. For the collapsed state, Solis et al. argue that the monomers and condensed counterions will behave as a homogeneous bulk state that is similar to an amorphous ionic solid.

To represent the free energy of the collapsed state, the distribution of charges in the collapsed state must first be determined. For a dense solid of fixed shape with mobile charges, the free mobile charges will tend to rearrange such that the excess charge is at the surface. For the pinned micelle model, this means that the center of the sphere is fully electroneutral, with the charge-compensating counterions canceling the monomer charge in that region. Any extra, uncompensated charges exist in a thin layer at the surface of the pinned micelle. This leads to an electrostatic free energy for the pinned micelle that is represented by a sum of the free energy of the core (F_{bulk}) and the charged surface (F_{cs}):

$$F_{elec} = F_{bulk} + F_{cs} \tag{11}$$

The energy for the charged surface is simple to represent in the same manner as the spherical cluster of charges used for the Zhulina approach and on a per chain basis:

$$\frac{F_{cs}}{kT} = l_B(fN)^2 n/R \tag{12}$$

In the core, all of the charges are in very close contact and the electrostatic interactions are strong. Thus, there is a very strong energetic penalty for configurations where a charge is not quickly compensated for by its neighbor. In some cases, this leads to crystallization, but the constraints due to connectivity of the chain may prevent that and the core can instead be represented by an amorphous ionic solid.[17]

For an ionic crystal, the energy per atom is

$$E_{eb} = -e^2\frac{M}{r_0} \tag{13}$$

DOI: 10.1021/acs.macromol.6b02563
Macromolecules XXXX, XXX, XXX−XXX

where r_0 is the lattice constant of the crystal and M is the Madelung constant, which allows for the calculation of the electric potential of all ions in a lattice felt by an ion at a specific position and is typically of the order 1. The overall energy of the crystal is determined by summing the interaction of one atom with all other atoms using a convergent series of alternating terms, summing the interaction of the atom with a layer of oppositely charged atoms that are the nearest neighbors, then with a layer of similarly charged ions that are the next-nearest neighbors, and so on.

To calculate the energy of the ionic solid, Solis et al. developed an estimate for the Madelung constant for the collapsed polymer. The simple estimate assumes a cluster of one counterion surrounded by all the monomers required to compensate its charge (one for monovalent and Z^+ for multivalent), assumes all distances are of the order a, and truncates the series at the first term.[17] This leads to an energy contribution for a cluster (i.e., for a single counterion in the collapsed core) of

$$\frac{E}{kT} = -l_B \frac{Z^+}{2}(Z^+ + 1) \tag{14}$$

The number of clusters (i.e., number of counterions in the collapsed core) is approximately equal to $(1 - f)Nn/Z^+$, so the electrostatic free energy of the bulk on a per chain basis is

$$\frac{F_{bulk}}{kT} = -l_B N\left(\frac{1}{2}(1 - f)(Z + 1)\right) \tag{15}$$

This term does not depend on "n", the number of tethers, so has no impact on the optimization to find the value of n at the minimum free energy. It does, however, impact the actual value of the free energy and is the primary contributor at the parameter values similar to those of the experiments.

Adaptation for Multivalent Ion-Driven Collapse. Thus far, we have focused primarily on the model for the polyelectrolyte brush collapse in a poor solvent with attractions driven by τ. In deriving a model for the electrostatics, we have only considered multivalent ions in the sense that they lead to the dense, amorphous ionic solid phase but have not included contributions for the attractions between chains due to bridging that would lead to a favorable collapsed state. Rather than including a distinct free energy term for the bridging attractions, we assume that the attractions are analogous to attractions in a poor solvent and describe a τ parameter that is dependent on the valence and strength of bridging rather than solvent quality.

For a first estimate for the contribution of bridging, we now define an effective poor solvent parameter, τ_{eff}, that will be used in the free energy equations for F_{surf} and F_{leg} and is dependent on the bridging parameter, g, and the valence of the counterion, Z^+. To estimate a form for τ_{eff}, we examine the virial term and the bridging term from the brush collapse equation we used for the homogeneous brush.[20]

$$\frac{1}{2}\tau\phi_m^{\,2} \quad \text{virial term} \tag{16}$$

$$g\phi_c(f\phi_m - \phi_c) \quad \text{bridging term} \tag{17}$$

where ϕ_c is the volume fraction of condensed counterions and ϕ_m is the volume fraction of monomers. To create an effective τ, we aim to produce a prefactor with a similar relationship to $\phi_m^{\,2}$ in the virial term, but based on the bridging interaction. If we assume $\phi_c/Z^+ \approx \phi_m$, then the bridging term becomes

$$\frac{g}{Z^+}\left(1 - \frac{1}{Z^+}\right)\phi_m^{\,2} \tag{18}$$

Thus, the effective τ parameter can be approximated by

$$\tau_{eff} = \frac{g}{Z^+}\left(1 - \frac{1}{Z^+}\right) \tag{19}$$

Cylindrical Bundle Structure. We hypothesize that the collapsed state of the brush may be as cylindrical bundles rather than pinned micelles for a polyelectrolyte brush due to the presence of free counterions, those that are not condensed. Cylinder formation is driven by the entropy gain from counterions in the more swollen cylinder state over the more collapsed spheres. This has been demonstrated for polyelectrolyte brushes in poor solvents through simulations by He et al., Sandberg et al., and Carrillo and Dobrynin.[27,28,31] These structures form in poor solvent conditions and moderate values of polymer charge.

The free energy of the bundle of polyelectrolyte chains can be described by the same sum of surface free energy, leg free energy, and electrostatic free energy (adjusted for the cylindrical geometry) as the pinned micelle model. Two additional terms must also be added for the bundle model: the osmotic free energy from the counterions and the elastic energy for the stretching of the chains.[31]

$$\frac{F_{bundle}}{kT} = \frac{F_{surf}}{kT} + \frac{F_{leg}}{kT} + \frac{F_{elec}}{kT} + \frac{F_{osm}}{kT} + \frac{F_{elast}}{kT} \tag{20}$$

With this new geometry, there are three size parameters as illustrated in Figure 2B (R, H, D) and the number of tethers to consider when minimizing the free energy. For D, the spacing between bundles, we can simply estimate D as a function of n:

$$D = \frac{nd}{2} \tag{21}$$

To relate the height, H, to the bundle radius, R, we assume that the bundles have a constant volume that depends on the number of tethers (i.e., that the monomer density is constant) and is based on the monomer density in the poor solvent:

$$V = \pi R^2 H \approx R_{poly}^{\,3} = nN/\tau \tag{22}$$

$$R = \left(\frac{nN}{\pi H \tau}\right)^{1/2} \tag{23}$$

This leaves us to minimize F_{bundle} with respect to only H and n.

The surface free energy for the bundles is assumed to be similar to that for the pinned micelles, but with a cylindrical geometry. The result is

$$\frac{F_{surf}}{kT} = 2\pi\gamma(RH + R^2) = 2\pi\frac{\tau^2}{n}(RH + R^2) \tag{24}$$

The deformation of the bundles is assumed to be similar to that for spherical structures, resulting in a leg stretching free energy of

$$F_{leg} = \tau n^{1/2} d \tag{25}$$

We can also assume the same representation of electrostatics as we did for the Zhulina model in the Pinned Micelle section. This assumes that the micelle core is essentially a cluster of

DOI: 10.1021/acs.macromol.6b02563
Macromolecules XXXX, XXX, XXX−XXX

individual charges, and we estimate the core as a charged liquid drop with Coulomb repulsion between charges. This results in

$$\frac{F_{elec}}{kT} = \frac{l_B(fN)^2 n}{H} \tag{26}$$

Similarly, using the amorphous ionic solid model[17] for the electrostatics that is similar to that from the pinned micelle geometry, we obtain

$$\frac{F_{cs}}{kT} = \frac{l_B(fN)^2 n}{H} \tag{27}$$

$$\frac{F_{bulk}}{kT} = -l_B N\left(\frac{1}{2}(1-f)(Z+1)\right) \tag{28}$$

In the cylindrical bundle representation, the free counterions are assumed to be within the brush volume, but between the cylinders. The condensed counterions are still assumed to be condensed on the chains within the bundles. This is illustrated in Figure 5:

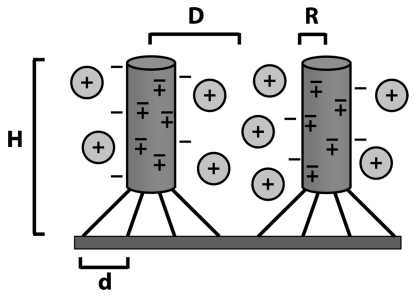

Figure 5. Illustration of cylindrical bundles with free counterions between the bundles.

The free counterions can thus contribute to the osmotic pressure and this must be considered in developing the model. The entropy of mixing of the counterions is

$$\phi_{ion} \ln \phi_{ion} \tag{29}$$

where ϕ_{ion} is the volume fraction of free counterions. The counterions are present in the volume

$$H(D^2 - R^2) \tag{30}$$

and the number of counterions in that volume is fnN/Z^+. This results in an osmotic free energy, on a per chain, per kT and per volume basis of

$$\frac{F_{osm}}{kT} = \frac{fN}{Z^+}\ln\left(\frac{fnN}{Z^+\pi H(D^2 - R^2)}\right) \tag{31}$$

The elastic stretching free energy contribution comes from the elastic stretching of the chains making up the core cylindrical aggregate. The equation for the free energy on a per chain basis is

$$\frac{F_{elast}}{kT} = \frac{3H^2}{2N} \tag{32}$$

This is similar to the elastic stretching in the homogeneous brush model:

$$\frac{F_{elast}}{kT} = \frac{L^2}{N} \tag{33}$$

This term will be minor when the structures are small (and hence negligible for the pinned micelle model) but will keep the bundles from becoming unreasonably tall.

RESULTS AND DISCUSSION

In this section, we will evaluate the different forms of the model for the collapsed brush, including the different representations for the electrostatics and the morphology of the collapsed state. We also will explore the impact of different parameter values and compare the results to experiments and the homogeneous brush model.

Pinned Micelle Structure. To investigate the feasibility of the pinned micelle model, we use a sum of the surface tension, leg stretching, and electrostatic free energy, with both the liquid drop and ionic solid electrostatics investigated. We minimize the free energy with respect to the number of legs, n, using numerical minimization functions in MATLAB and determine the approximate pinned micelle size (recall $R = (nN/\tau)^{1/3}$). There are multiple parameters based on experimental conditions that must be defined for each set of results including the grafting spacing, d, the number of monomers, N, and the valence of the counterions, Z^+. Unless otherwise specified, we select $d = 20$, $N = 1000$, and $Z^+ = 3$ based on reasonable values in the experimental literature.[10,12] We also select a baseline value for the bridging parameter, $g = 4$, which leads to a value of $\tau = 0.9$.

The brush height (twice the micelle radius), number of legs, and the minimum value of the free energy for the pinned micelle model at different values of the remaining charge fraction are shown in Table 1. These estimates for the micelle

Table 1. Equilibrum Number of Chains, Brush Height, and Minimum Free Energy for the Pinned Micelle Model at d = 20, N = 1000, Z^+ = 3, g = 4, and f = 0.9, 0.1, 0.01, and 0

remaining polymer charge	parameter	liquid drop F_{elec}	ionic solid F_{elec}
$f = 0.9$	n	0.0002	0.0002
	$2R$	0.3 nm	0.3 nm
	F_{min}	2210	1650
$f = 0.1$	n	0.02	0.02
	$2R$	1.3 nm	1.3 nm
	F_{min}	512	−4530
$f = 0.01$	n	1.1	1.1
	$2R$	5.3 nm	5.3 nm
	F_{min}	130	−5410
$f = 0$	n	4.0	4.0
	$2R$	8.2 nm	8.2 nm
	F_{min}	89	−5510

radius are still lower than measured experimentally (~30 nm), but the estimates for the lower brush charge fractions, 5.3 and 8.2 nm for $f = 0.01$ and 0, respectively, are much closer than the estimate with the homogeneous brush model (~0.07 nm).

The fraction of charges remaining on the polymer after counterion condensation, f, has a strong effect on the brush height, number of chains in the pinned micelle, and minimum free energy. Using the simple Manning theory, where the fraction of condensed counterions is $\theta \approx 1 - 1/(Z^+ l_B/a)$,[32] we can estimate that for trivalent ions the fraction of condensed counterions is approximately 90%. Experimental results have consistently indicated higher levels of counterion condensation, however, and an accurate theoretical prediction is still an active research area. We, therefore choose four values of the

DOI: 10.1021/acs.macromol.6b02563
Macromolecules XXXX, XXX, XXX−XXX

remaining charge fraction: one that is very high (f = 0.9), indicating little counterion condensation, one that corresponds to Manning's prediction (f = 0.1), one that is low (f = 0.01), indicating very high counterion condensation, and f = 0, corresponding to all charges being neutralized in the collapsed state.

For f = 0.9 and 0.1, the results are unphysical, with far less than one chain per pinned micelle. At such high charge fractions, there would a significant amount of charge repulsion in a dense state, so the chains would be more likely to be in an extended state. This is consistent with prediction in Zhulina et al. that the crossover from collapsed to extended brush in a poor solvent would occur at $f \approx 0.02$.[23] When we use a charge fraction lower than that indicating a high degree of counterion condensation, the number of chains in a pinned micelle becomes greater than 1 and the brush height rises. For f = 0, indicating complete neutralization of the polyelectrolyte chain by condensed counterions, the equilibrium number of chains is 4 and the brush height is 8.2 nm, the closest to the experimentally measured brush height, approximately 30 nm.

The results of the model are the most realistic at very high levels of counterion condensation. There is significant evidence that this is a valid assumption for polyelectrolytes with multivalent ions. Experimental studies on polyelectrolytes in solution have shown that a majority of the multivalent ions are very near the polymer chain at the point just before collapse, indicating that they are likely condensed.[33,34] Additional studies have shown that in the collapsed state all multivalent ions are near the polymer chain, indicating a dense structure with multivalent ions neutralizing the polymer charges.[35] Simulations of polyelectrolyte brushes with multivalent ions have also shown that the collapsed state is essentially neutralized.[36,37] Given the evidence in the literature and the supporting model results here, we will consider only charge fractions f = 0.01 and f = 0 going forward.

Table 1 contains results for both representations of the electrostatics: the liquid drop[23] and the ionic solid.[17] The equilibrium number of chains and brush height for the pinned micelle do not depend on the method used for the electrostatics, but the minimum value of the free energy is very different in the two cases. F_{min} is much lower for the ionic solid method, which is expected since the method adds a term that makes it more favorable to have the opposite charges near one another in the collapsed state.

A final observation can be made from the results in Table 1. The equilibrium number of chains in a pinned micelle is low, even for the cases with low remaining charge fractions. One reason for this may be that the grafting density is low and the brush may be in the mushroom regime, where a single globule would form per chain. It is thus important to examine the behavior of the brush for a range of grafting densities. Table 2 shows the equilibrium number of chains and brush height for four different values of the grafting spacing. The equilibrium number of chains does increase as the grafting spacing decreases (density increases); however, it is not a large effect for f = 0.01. For f = 0, the equilibrium number of chains in the pinned micelle increases from 1.8 to 21 as d is decreased from 40 to 5. These results indicate that grafting density does play a role, but when uncompensated charges are present on the polyelectrolyte chain, the charge repulsion is the stronger effect and keeps the number of chains in the pinned micelle low.

The effect of multivalent ions enters through the τ parameter, defined in eq 19 as a function of Z^+ and a parameter for the strength of bridging, g, and analogous to the τ parameter for solvent quality. Table 3 shows the equilibrium number of chains and brush height for various values of the τ parameter. As the bridging becomes more favorable (the effective solvent quality worsens), the number of chains in the pinned micelle increases and the size of the pinned micelle decreases. This is because, as we increase the tendency for attractions between chains, it is more favorable for a greater number of chains to be in the micelle, but the density of the monomers in the collapsed state also decreases due to these additional attractions, leading to smaller pinned micelles.

Table 2. Equilibrium Number of Chains and Brush Height for the Pinned Micelle Model at N = 1000, Z^+ = 3, g = 4, f = 0.01 and 0, and d = 40, 20, 10, and 5

grafting spacing, d	parameter	value (at f = 0.01)	value (at f = 0)
40	n	0.8	1.8
	$2R$	4.8 nm	6.2 nm
20	n	1.1	4.0
	$2R$	5.3 nm	8.2 nm
10	n	1.3	9.3
	$2R$	5.6 nm	10.8 nm
5	n	1.4	21
	$2R$	5.8 nm	14.4 nm

Table 3. Equilibrium Number of Chains and Brush Height for the Pinned Micelle Model at d = 20, N = 1000, Z^+ = 3, f = 0.01 and 0, and g = 2, 4, 6, and 8

τ	parameter	value (at f = 0.01)	value (at f = 0)
0.4 (g = 2)	n	0.6	3.0
	$2R$	6.4 nm	9.4 nm
0.9 (g = 4)	n	1.1	4.0
	$2R$	5.3 nm	8.2 nm
1.3 (g = 6)	n	1.5	4.8
	$2R$	5.2 nm	7.6 nm
1.8 (g = 8)	n	1.9	5.3
	$2R$	5.0 nm	7.2 nm

Cylindrical Bundle Structure. For the cylindrical bundle model, we assume a geometry where the chains form pillars of height H, radius R, and spacing between pillars of D. Many counterions are condensed on the chains in the dense pillars, lowering the effective polymer charge fraction to f, and any remaining counterions are trapped in the brush volume but free to move between the pillars. We define the key parameters d = 20, N = 1000, and Z^+ = 3 based on reasonable values in the experimental literature.[10,12] We also select a baseline value for the bridging parameter, g = 4, which leads to a value of τ = 0.9. The free energy was minimized with respect to the brush height and number of chains, with the values of R and D set by eqs 23 and 21, respectively, and the results are presented in Table 4.

At high charge fractions, the equilibrium brush height is very high and the number of chains in the bundle is low. This is due to the strong contribution to the free energy from the entropy of the free counterions, which is able to overcome the elastic stretching penalty and the increase of the surface area. At the lower charge fraction of f = 0.01, where there is a higher degree of counterion condensation, the brush height is still higher than that for the pinned micelle model, 13.3 nm compared to 5.3 nm, due to the contribution from the free counterions, but they have a much lower effect. And for the completely neutralized brush, the brush height is virtually the same, 8.4 nm compared

DOI: 10.1021/acs.macromol.6b02563
Macromolecules XXXX, XXX, XXX−XXX

Table 4. Equilibrium Number of Chains, Brush Height, and Minimum Free Energy for the Cylindrical Bundle Model at d = 20, N = 1000, Z^+ = 3, g = 4, and f = 0.9, 0.1, 0.01, and 0

remaining polymer charge	parameter	result
f = 0.9	n	0.4
	H	113 nm
	F_{min}	3360
f = 0.1	n	2.2
	H	37 nm
	F_{min}	−4050
f = 0.01	n	12.8
	H	13.3 nm
	F_{min}	−5221
f = 0	n	31
	H	8.4 nm
	F_{min}	−5350

to 8.2 nm, with the difference arising from inclusion of the elastic stretching term in the bundle model. This indicates that the bundle model may provide a more realistic representation for the system at lower levels of counterion condensation, provided that the free counterions remain within the brush volume.

For systems with multivalent counterions and no added salt, as are represented in the models discussed here, counterion condensation is expected to be very high, and there are very few free counterions to contribute to stretching. Comparing the minimum value of the free energy found for the pinned micelle model at f = 0.01, −5410, to the value for the cylindrical bundle at the same charge fraction, −5221, we see that the pinned micelle model has the lower free energy and would be favored. This is in contrast to a system such as that discussed in Carrillo and Dobrynin with the polyelectrolyte brush in a poor solvent with monovalent counterions, where there are more free counterions to contribute to the osmotic pressure and make the bundle configuration more favorable than a pinned micelle configuration at some conditions.[27]

Since many practical systems of interest occur in the presence of added salt and mixtures of mono- and multivalent ions, we aim to explore this further. Though it is beyond the scope of this simple model to accurately predict the proportion of free counterions in the space between the bundles in the presence of added salt, we can determine the effect of increasing the number of these free counterions on the model results. To do this, we add an additional osmotic term to the overall free energy of the cylindrical bundles to account for extra counterions.

$$\frac{F_{osm,ex}}{kT} = \beta f N \ln\left(\frac{\beta f n N}{\pi H(D^2 - R^2)}\right) \quad (34)$$

where β is a multiplier to adjust the number of extra free ions in the brush, i.e., the ratio of the number of excess ions to the number of free counterions. To compare the bundle model to the pinned micelle model in this case, we add F_{osm}, F_{elas}, and $F_{osm,ex}$ to the pinned micelle model, maintaining the spherical geometry of that system, which has a volume of $8Rnd^2$ between the pinned micelles where the counterions are free.

$$\frac{F_{osm}}{kT} = \frac{fN}{Z^+}\ln\left(\frac{fnN}{8Z^+Rnd^2}\right) \quad (35)$$

$$\frac{F_{elast}}{kT} = \frac{2R^2}{2N} \quad (36)$$

$$\frac{F_{osm,ex}}{kT} = \beta f N \ln\left(\frac{\beta f n N}{8Rnd^2}\right) \quad (37)$$

We calculate the minimum value of the free energy for various values of β at a remaining charge fraction of f = 0.01 for both the cylindrical bundle model and the modified pinned micelle model. Figure 6 shows these results and that there is a clear change in which model is more favorable as β is increased. At β of approximately 10, the bundle model becomes more favorable due to the extra space available for the free counterions. Though this is not readily relatable to experimental results due to the simplification in how many free ions are in the brush volume between the structures, it does point to a potential physical situation in which cylindrical bundles may form and serves as a starting point for a model of mixtures of monovalent and multivalent ions in these systems.

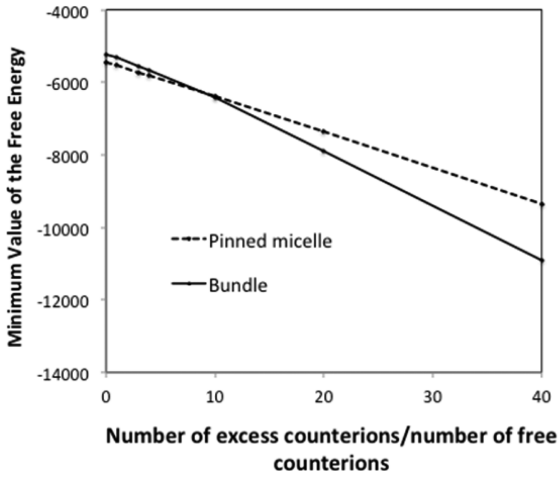

Figure 6. Minimum value of the free energy as a function of β, the ratio of the number of excess counterions to the number of free counterions.

Evaluation of Poor Solvent Analogy. The models presented here assume that the attractions between polymer chains leading to collapse are analogous to attractions between monomers in a poor solvent, with the magnitude of the attraction, characterized by the τ parameter, as an open parameter that could relate to bridging attractions. We have shown that the lateral inhomogeneities seen for polymer and polyelectrolyte brushes in poor solvents are consistent with current experimental results for the collapsed brush, in that the predicted brush height is consistent with measurements made via surface force apparatus and neutron reflectivity.[10,13] It is expected that the collapse results from short-range attractions, but the nature of these attractions is a point of discussion. There are two potential mechanisms for collapse, neutralization and electrostatic bridging, and it is important to clarify which is the primary driver for this phenomenon.

Multivalent ions are known to associate more readily to the polyelectrolyte chain than monovalent ions and result in a very high level of counterion condensation. One hypothesis for the collapse is that the brush collapses when the amount of multivalent counterions is sufficient to neutralize (or nearly neutralize) the polymer chains. This reduces the chain

DOI: 10.1021/acs.macromol.6b02563
Macromolecules XXXX, XXX, XXX−XXX

solubility significantly since the polymer backbone is typically poorly soluble and leads to short-range attractions between monomers and collapse as with other polymer brushes in poor solvents.

For the second contribution to attractions between chains leading to collapse, electrostatic bridging can arise from a single multivalent ion condensing onto two monomers of the polymer chain, forming an ionic bridge. In addition to bridging, dipole−dipole interactions from counterions condensed on the brush strands would also contribute to the electrostatic attractions between polymer chains, particularly in mixtures of multivalent and monovalent ions, where both types would be condensed. This has been studied for polyelectrolytes in monovalent ion solutions, with particular focus on counterion correlation induced attractions leading to necklace, globule, or other structure formation.[21,38,39] For this electrostatic bridging hypothesis, it is supposed that the attractions between chains due to electrostatics, primarily direct ionic bridging, are what drive the brush collapse.

One of the primary arguments for the neutralization-driven collapse hypothesis is that in simulations the structure is fully collapsed at the charge match point, where the number of charges from the multivalent counterions equals those of the polyelectrolyte chains.[37] Experimental studies on polyelectrolytes in multivalent ionic solutions have also shown that a majority of the ions are very near the polymer chain at the point just before collapse, indicating that they are likely condensed.[33,34] Additional studies have shown that in the collapsed state all multivalent ions are near the polymer chain, indicating a dense structure with multivalent ions neutralizing the polymer charges.[35]

In considering the bridging effect in polyelectrolyte collapse, it is valuable to start by examining collapse of polyelectrolytes in the presence of monovalent ions. At low temperatures, there is an increase in counterion condensation in monovalent ionic solutions and collapse of the polyelectrolyte chain, shown in simulation[40] and examined in theory.[21,41] The collapse is explained not by neutralization of the chain, but by attractions between different parts of the chain due to short-range dipole−monomer and dipole−dipole interactions. These interactions are described as similar to poor solvent behavior with an effective second virial coefficient that depends on the condensed counterions.[21] This makes the hypothesis consistent with the observations that the polyelectrolyte brush collapsed structure is similar to that for a brush in a poor solvent but with a driving mechanism that is based in electrostatics.

For systems with multivalent ions, the attractions will be stronger than the case of condensed monovalent ions due to the bridging effect. This could lead to collapse of the polymer chain at lower concentrations of multivalent ions, as was observed in Olvera de la Cruz et al., where precipitation from solution was observed at a trivalent ion:polymer concentration ratio of 0.23.[15] Neutralization would be expected to occur at a ratio of 0.33 for trivalent ions, so the experimentally observed collapse occurs below the neutralization point. Theoretical predictions using electrostatic attraction between negatively charged bare monomers and "positively charged" monomers containing a condensed multivalent counterion (i.e., the bridging effect) fit well with the experimental data in polyelectrolyte solutions.[15] These results indicate that collapse could, indeed, be driven by electrostatic attractions from ionic bridging; however, they are not fully conclusive due to complications in knowing the precise amount of counterion condensation and accounting for competition between ionic species.

A strong argument for bridging-driven collapse of polyelectrolytes in multivalent ionic solutions was made in a simulation study that examined not only the parameters leading to collapse but also the dynamics of the collapse.[42] They showed that in a theta solvent for the neutral polymer chain collapse of the polyelectrolyte still occurs for trivalent ionic solutions. This is strong evidence that electrostatic interactions through condensed counterions contribute to the collapse, though does not necessarily mean that it is the strongest mechanism when the chain is in a poor solvent for the backbone and the two mechanisms may compete.

At this point, there is evidence in support of both mechanisms for collapse and the lateral inhomogeneities predicted in these models are consistent with both hypotheses, as they are both based on short-range attractions overcoming the long-range electrostatic repulsion. Further work in understanding the mechanism driving the collapse could lead to a more precise representation of bridging than the parametrized τ used here.

CONCLUSIONS

In this work, we have adapted a model for polyelectrolyte brush collapse in poor solvents to represent polyelectrolyte brush collapse in the presence of multivalent ions. We have assumed that the attractions between chains due to multivalent ions, whether caused directly by ionic bridging or by neutralization of chains, are analogous to attractions in poor solvents and have used a sum of the surface tension, leg stretching and electrostatic free energies, with an effective poor solvent parameter based on the ion valence and the strength of the attraction. The model considers two potential structures for the resulting collapsed state, the pinned micelle and cylindrical bundle, with equilibrium brush heights at f = 0.01 of 5.3 and 13.3 nm, respectively. By allowing for lateral inhomgeneities in the collapsed state, we find brush heights that are much closer to the experimentally measured brush height of approximately 30 nm than was previously seen with a homogeneous collapse model (0.07 nm).[20] Understanding the formation of lateral structures during multivalent ion-driven collapse is important for fundamental studies of how polyelectrolytes interact with multivalent ions. It is also extremely valuable for predicting behavior of polyelectrolyte brushes in many applications due to the presence of multivalent ions in many industrial formulations and biological fluids and can even be used to design new stimuli-responsive materials with nanoscale structure such as patchy particles.[5] The simple model described here provides a foundation for predicting lateral structure formation and understanding the collapse of the polyelectrolyte brush and can serve as a starting point for elucidating the mechanism driving collapse and developing experimental and simulation work to more fully understand the collapsed state in simple, as well as more complex systems, such as those with added salt, mixtures of multivalent and monovalent ions, proteins, and other polyelectrolytes.

AUTHOR INFORMATION

Corresponding Author

*E-mail mtirrell@uchicago.edu (M.T.).

ORCID

Blair Brettmann: 0000-0003-1335-2120

DOI: 10.1021/acs.macromol.6b02563
Macromolecules XXXX, XXX, XXX−XXX

Notes

The authors declare no competing financial interest.

■ ACKNOWLEDGMENTS

This work was supported by the U.S. Department of Energy Office of Science, Program in Basic Energy Sciences, Materials Sciences and Engineering Division. The authors thank Changbong Hyeon, Nicholas Jackson, and Jing Yu for helpful discussions.

■ REFERENCES

(1) Pincus, P. Colloid stabilization with grafted polyelectrolytes. *Macromolecules* **1991**, *24* (10), 2912−2919.
(2) Klein, J.; Kamiyama, Y.; Yoshizawa, H.; et al. Lubrication forces between surfaces bearing polymer brushes. *Macromolecules* **1993**, *26* (21), 5552−5560.
(3) Minko, S. Responsive Polymer Brushes. *J. Macromol. Sci., Polym. Rev.* **2006**, *46* (4), 397−420.
(4) Azzaroni, O. Polymer brushes here, there, and everywhere: Recent advances in their practical applications and emerging opportunities in multiple research fields. *J. Polym. Sci., Part A: Polym. Chem.* **2012**, *50* (16), 3225−3258.
(5) Choueiri, R. M.; Galati, E.; Thérien-Aubin, H.; Klinkova, A.; Larin, E. M.; Querejeta-Fernández, A.; Han, L.; Xin, H. L.; Gang, O.; Zhulina, E. B.; et al. Surface patterning of nanoparticles with polymer patches. *Nature* **2016**, *538* (7623), 79−83.
(6) Schneck, E.; Papp-Szabo, E.; Quinn, B. E.; Konovalov, O. V.; Beveridge, T. J.; Pink, D. A.; Tanaka, M. Calcium ions induce collapse of charged O-side chains of lipopolysaccharides from Pseudomonas aeruginosa. *J. R. Soc., Interface* **2009**, *6*, S671−S678.
(7) Attili, S.; Borisov, O. V.; Richter, R. P. Films of End-Grafted Hyaluronan Are a Prototype of a Brush of a Strongly Charged, Semiflexible Polyelectrolyte with Intrinsic Excluded Volume. *Biomacromolecules* **2012**, *13* (5), 1466−1477.
(8) Borisov, O. V.; Birshtein, T. M.; Zhulina, E. Collapse of grafted polyelectrolyte layer. *J. Phys. II* **1991**, *1*, 521−526.
(9) Rühe, J.; Ballauff, M.; Biesalski, M.; Dziezok, P.; Gröhn, F.; Johannsmann, D.; Houbenov, N.; Hugenberg, N.; Konradi, R.; Minko, S.; et al. Polyelectrolyte Brushes. In *Polyelectrolyte Complexes in the Dispersed and Solid State I*; Advances in Polymer Science; Springer: Berlin, 2004; Vol. *165*, pp 79−150.
(10) Farina, R.; Laugel, N.; Pincus, P.; Tirrell, M. Brushes of strong polyelectrolytes in mixed mono- and tri-valent ionic media at fixed total ionic strengths. *Soft Matter* **2013**, *9* (44), 10458−16.
(11) Farina, R.; Laugel, N.; Yu, J.; Tirrell, M. Reversible Adhesion with Polyelectrolyte Brushes Tailored via the Uptake and Release of Trivalent Lanthanum Ions. *J. Phys. Chem. C* **2015**, *119* (26), 14805−14814.
(12) Yu, J.; Mao, J.; Yuan, G.; Satija, S.; Jiang, Z.; Chen, W.; Tirrell, M. Structure of Polyelectrolyte Brushes in the Presence of Multivalent Counterions. *Macromolecules* **2016**, *49* (15), 5609−5617.
(13) Yu, J.; Mao, J.; Yuan, G.; Satija, S.; Chen, W.; Tirrell, M. The effect of multivalent counterions to the structure of highly dense polystyrene sulfonate brushes. *Polymer* **2016**, *98* (C), 448−453.
(14) Mei, Y.; Lauterbach, K.; Hoffmann, M.; Borisov, O. V.; Ballauff, M.; Jusufi, A. Collapse of Spherical Polyelectrolyte Brushes in the Presence of Multivalent Counterions. *Phys. Rev. Lett.* **2006**, *97* (15), 158301−158304.
(15) de la Cruz, M. O.; Belloni, L.; Delsanti, M.; Dalbiez, J. P.; Spalla, O.; Drifford, M. Precipitation of highly charged polyelectrolyte solutions in the presence of multivalent salts. *J. Chem. Phys.* **1995**, *103* (13), 5781−5791.
(16) Hsiao, P.-Y.; Luijten, E. Salt-Induced Collapse and Reexpansion of Highly Charged Flexible Polyelectrolytes. *Phys. Rev. Lett.* **2006**, *97* (14), 148301−148304.
(17) Solis, F. J.; de la Cruz, M. O. Collapse of flexible polyelectrolytes in multivalent salt solutions. *J. Chem. Phys.* **2000**, *112* (4), 2030−2035.
(18) Jusufi, A.; Borisov, O.; Ballauff, M. Structure formation in polyelectrolytes induced by multivalent ions. *Polymer* **2013**, *54* (8), 2028−2035.
(19) Plamper, F. A.; Walther, A.; Müller, A.; Ballauff, M. Nanoblossoms: light-induced conformational changes of cationic polyelectrolyte stars in the presence of multivalent counterions. *Nano Lett.* **2007**, *7* (1), 167−171.
(20) Brettmann, B. K.; Laugel, N.; hoffmann, N.; Pincus, P.; Tirrell, M. Bridging contributions to polyelectrolyte brush collapse in multivalent salt solutions. *J. Polym. Sci., Part A: Polym. Chem.* **2016**, *54* (2), 284−291.
(21) Schiessel, H.; Pincus, P. Counterion-Condensation-Induced Collapse of Highly Charged Polyelectrolytes. *Macromolecules* **1998**, *31* (22), 7953−7959.
(22) Williams, D. R. M. Grafted polymers in bad solvents: octopus surface micelles. *J. Phys. II* **1993**, *3* (9), 1313−1318.
(23) Zhulina, E.; Singh, C.; Balazs, A. C. Behavior of tethered polyelectrolytes in poor solvents. *J. Chem. Phys.* **1998**, *108* (3), 1175−10.
(24) Bracha, D.; Bar-Ziv, R. H. Dendritic and Nanowire Assemblies of Condensed DNA Polymer Brushes. *J. Am. Chem. Soc.* **2014**, *136* (13), 4945−4953.
(25) Yeung, C.; Balazs, A. C.; Jasnow, D. Lateral instabilities in a grafted layer in a poor solvent. *Macromolecules* **1993**, *26* (8), 1914−1921.
(26) Ross, R. S.; Pincus, P. Bundles: End-Grafted Polymer Layers in Poor Solvent. *Europhys. Lett.* **1992**, *19* (2), 79−84.
(27) Carrillo, J.-M. Y.; Dobrynin, A. V. Morphologies of Planar Polyelectrolyte Brushes in a Poor Solvent: Molecular Dynamics Simulations and Scaling Analysis. *Langmuir* **2009**, *25* (22), 13158−13168.
(28) He, G.-L.; Merlitz, H.; Sommer, J.-U. Molecular dynamics simulations of polyelectrolyte brushes under poor solvent conditions: Origins of bundle formation. *J. Chem. Phys.* **2014**, *140* (10), 104911−104913.
(29) Halperin, A.; Zhulina, E. B. On the Deformation Behaviour of Collapsed Polymers. *Europhys. Lett.* **1991**, *15* (4), 417−421.
(30) Zhulina, E. B.; Birshtein, T. M.; Priamitsyn, V. A.; Klushin, L. I. Inhomogeneous structure of collapsed polymer brushes under deformation. *Macromolecules* **1995**, *28* (25), 8612−8620.
(31) Sandberg, D. J.; Carrillo, J.-M. Y.; Dobrynin, A. V. Molecular Dynamics Simulations of Polyelectrolyte Brushes: From Single Chains to Bundles of Chains. *Langmuir* **2007**, *23* (25), 12716−12728.
(32) Manning, G. S. Limiting Laws and Counterion Condensation in Polyelectrolyte Solutions I. Colligative Properties. *J. Chem. Phys.* **1969**, *51* (3), 924−11.
(33) Sabbagh, I.; Delsanti, M.; Lesieur, P. Ionic distribution and polymer conformation, near phase separation, in sodium polyacrylate/divalent cations mixtures: small angle X-ray and neutron scattering. *Eur. Phys. J. B* **1999**, *12* (2), 253−260.
(34) Schweins, R.; Goerigk, G.; Huber, K. Shrinking of anionic polyacrylate coils induced by Ca2+, Sr2+ and Ba2+: A combined light scattering and ASAXS study. *Eur. Phys. J. E: Soft Matter Biol. Phys.* **2006**, *21* (2), 99−110.
(35) Angelini, T. E.; Sanders, L. K.; Liang, H.; Wriggers, W.; Tang, J. X.; Wong, G. C. L. Structure and dynamics of condensed multivalent ions within polyelectrolyte bundles: a combined x-ray diffraction and solid-state NMR study. *J. Phys.: Condens. Matter* **2005**, *17* (14), S1123−S1135.
(36) Mei, Y.; Hoffmann, M.; Ballauff, M.; Jusufi, A. Spherical polyelectrolyte brushes in the presence of multivalent counterions: The effect of fluctuations and correlations as determined by molecular dynamics simulations. *Phys. Rev. E* **2008**, *77* (3), 031805−031810.
(37) Guptha, V. S.; Hsiao, P.-Y. Polyelectrolyte brushes in monovalent and multivalent salt solutions. *Polymer* **2014**, *55* (12), 2900−2912.
(38) Dobrynin, A. V.; Rubinstein, M. Counterion condensation and phase separation in solutions of hydrophobic polyelectrolytes. *Macromolecules* **2001**, *34* (6), 1964−1972.

DOI: 10.1021/acs.macromol.6b02563
Macromolecules XXXX, XXX, XXX−XXX

(39) Liao, Q.; Dobrynin, A. V.; Rubinstein, M. Counterion-correlation-induced attraction and necklace formation in polyelectrolyte solutions: Theory and simulations. *Macromolecules* **2006**, *39* (5), 1920−1938.
(40) Winkler, R.; Gold, M.; Reineker, P. Collapse of Polyelectrolyte Macromolecules by Counterion Condensation and Ion Pair Formation: A Molecular Dynamics Simulation Study. *Phys. Rev. Lett.* **1998**, *80* (17), 3731−3734.
(41) González-Mozuelos, P.; de la Cruz, M. O. Ion condensation in salt-free dilute polyelectrolyte solutions. *J. Chem. Phys.* **1995**, *103* (8), 3145−3157.
(42) Lee, N.; Thirumalai, D. Dynamics of Collapse of Flexible Polyelectrolytes in Poor Solvents. *Macromolecules* **2001**, *34* (10), 3446−3457.

DOI: 10.1021/acs.macromol.6b02563
Macromolecules XXXX, XXX, XXX−XXX